

Solution-Based Suspension Synthesis of $\text{Li}_2\text{S}-\text{P}_2\text{S}_5$ Glass-Ceramic Systems as Solid-State Electrolytes: A Brief Review of Current Research

Zachary Warren and Nataly Carolina Rosero-Navarro*



Cite This: *ACS Omega* 2024, 9, 31228–31236



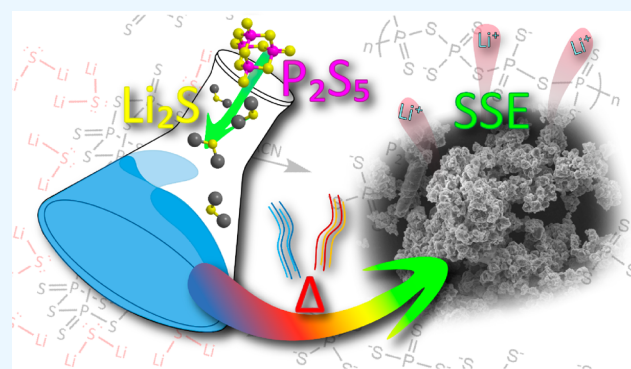
Read Online

ACCESS |

Metrics & More

Article Recommendations

ABSTRACT: All-solid-state batteries are set to be the next generation of batteries offering improved performance and safety over current conventional lithium-ion batteries. Glass-ceramic $\text{Li}_2\text{S}-\text{P}_2\text{S}_5$ solid-state sulfide electrolytes are promising contenders to achieve all-solid-state batteries with exceptional ionic conductivity on the order of $10^{-2} \text{ S cm}^{-1}$. Solid-state processing techniques for synthesizing sulfide solid electrolytes are energetically and time consumptive. However, proposed solution processing techniques offer faster and lower temperature processes rendering them scalable. The chemistries that underly solution processing of sulfide solid electrolytes are still not well understood. This brief review highlights key aspects of current research into solution-based suspension synthesis processing techniques of $\text{Li}_2\text{S}-\text{P}_2\text{S}_5$ sulfide solid electrolytes discussing precursor stoichiometries, solvent selectivity, reaction conditions, chemical impurities, and particle morphology with the intent of promoting further research into solution processing of sulfide solid-state electrolytes.



1. INTRODUCTION

The pursuit of high-performing and sustainable energy storage solutions for electric vehicle transportation has placed solid-state batteries at the forefront of battery research, offering a safer alternative to conventional lithium-ion batteries. Current conventional batteries, when damaged or malfunctioned, are known to suffer thermal runaway, fire, or explosion posing a serious hazard to health and safety. Among the contributors to battery fires, high energy electrode materials in combination with organic liquid electrolytes are generally to blame. It has been considered that replacing liquid electrolytes with nonflammable solid-state electrolytes can offer enhanced safety to overall battery performance.

Sulfide solid electrolytes (SSEs) have gained much significance in the field of solid-state battery research in the past decade due to their remarkable electrochemical and mechanical properties. In 2011, Kamaya et al. reported the synthesis of the lithium superionic conductor SSE $\text{Li}_{10}\text{GeP}_2\text{S}_{12}$ (LGPS) with an ionic conductivity of 12 mS cm^{-1} at room temperature.¹ Two years later in 2013, Tatsumisago et al. reported an SSE with ionic conductivity of 17 mS cm^{-1} at room temperature, which was attributed to the crystallization of $\text{Li}_7\text{P}_3\text{S}_{11}$ in the binary $\text{Li}_2\text{S}-\text{P}_2\text{S}_5$ (LPS) system.² The SSE $\text{Li}_{9.54}\text{Si}_{1.74}\text{P}_{1.44}\text{S}_{11.7}\text{Cl}_{0.3}$ was reported to have an ionic conductivity of an astonishing 25 mS cm^{-1} by Kato et al. and still retained the LGPS-like structure.³ Subsequent

mechanical evaluations of LPS SSEs have reported favorable Young's moduli which are appealing for solid-state battery materials. Accordingly, these electrochemical and mechanical properties have placed SSEs in the forefront of solid-state battery research.

With such favorable characteristics, processing methods to develop and enhance SSEs have been widely investigated. The LGPS and LPS systems discussed were both synthesized in highly energetic solid-state processes. The LGPS system synthesized by Kato et al. was mechanically ball milled for 40 h then annealed for 8 h at high temperature,³ while the LPS system reported by Tatsumisago et al. was synthesized by melt-quenching at $700 \text{ }^\circ\text{C}$.² Both of these reported processes are commonplace in SSE research, however they present significant obstacles when developing scalable processes that could render SSEs commercially viable. High-energy and low throughput processes, such as solid-state synthesis of SSEs, have a negative impact on the manufacturing costs and solid-state battery production.

Received: April 19, 2024

Revised: June 7, 2024

Accepted: June 26, 2024

Published: July 9, 2024



The first report of a solution-based process for LPS systems was published in 2013 by Liu et al. coinciding with the report of the superionic conductor of LPS.² Liu et al.'s reported solution process was conducted using the LPS system in tetrahydrofuran (THF) and synthesized an SSE with ionic conductivity of 0.16 mS cm^{-1} , which was identified as β - Li_3PS_4 .⁴ In the same year, Tatsumisago et al. reported the solution of an LPS system in *N*-methylformamide (NMF) while investigating methods to improve the electrode-SSE interface⁵ and Huang et al. reported a similar solution process for an LGPS using hydrazine.⁶ Inevitably, the characteristic solubility of Tatsumisago's SSE in NMF led to the solution-based suspension synthesis of LPS in NMF and *n*-hexane, forming Li_3PS_4 with ionic conductivity of $2.3 \times 10^{-6} \text{ S cm}^{-1}$.⁷ In the wake of Liu et al.'s pioneering work on SSE processing with THF, followed by Tatsumisago et al.'s investigations with NMF and Huang et al.'s LGPS synthesis using hydrazine, a novel field of research has emerged: the solution-based processing of SSEs.

These initial approaches to SSE processing using solvents illustrate a divergence in solution-based processing techniques, from dissolution–precipitation to suspension synthesis processes in which involve reacting precursor reagents in a solvent. Solution-based dissolution–precipitation processes have been used for SSE deposition and the coating of active materials while suspension syntheses have enabled the synthesis of different SSEs. This divergence is notably important when distinguishing the similarities and differences between the types of solution-based processes. Solution-based processing of SSEs is a broad field of techniques that encapsulate all the processes that can be performed using a solid electrolyte and a solvent or mixture of solvents. Solution-based processing includes both solution-based dissolution–precipitation techniques and solution-based suspension synthesis techniques.

Since the initial experiments of solution-based processing of SSEs until now, there have been reports of solution-based suspension synthesis of LPS systems that have reached ionic conductivities of 3.1 mS cm^{-1} ¹⁸ and $\text{Li}_6\text{PS}_5\text{Cl}$ (LPSC) systems of up to 4.3 mS cm^{-1} ¹⁹ at room temperature. Various reports have been released about the influence on LPS systems from molar stoichiometries of precursor reagents, solvents used, and chemical impurities that affect the overall performance of the synthesized SSEs. Regardless of the published reports, there is a lack of information regarding the effects of solvent properties on these chemical reactions and how solvents facilitate the formation of SSEs. To date, research into LPS SSE solution-based suspension synthesis is only moderately progressing and holds paramount to the future of SSEs.

This review assesses key factors related to the solution-based suspension synthesis of LPS SSEs with the intent of promoting investigation into the chemistries that facilitate these reactions. We opted to concentrate on solution-based suspension synthesis instead of dissociation–precipitation solution process because the former is expected to play a more significant role in the synthetic processes influencing the production of SSEs. Additionally, we selected the LPS system over LGPS and LPSX ($X = \text{I, Cl, or Br}$), due to simplicity of the binary system of LPS. With a more complete understanding of the reaction chemistries that facilitate the synthesis of binary LPS SSEs and the reactions between Li_2S and P_2S_5 in solvent, a foundation of information can support further research into other complex systems such as LGPS and LPSX SSEs. Ultimately, despite the LPS system's ability to provide SSEs with high ionic

conductivity, the underlying reaction mechanisms for solution-based suspension synthesis remain unclear.

2. SOLUTION-BASED SUSPENSION SYNTHESIS

A simple solution-based suspension synthesis for LPS SSEs can be categorized into three steps: (1) solvent-facilitated reaction, (2) solvent removal, and (3) SSE annealing as seen in Figure 1.

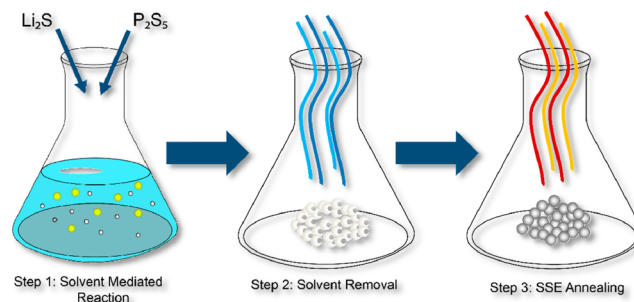


Figure 1. Solution-based suspension synthesis.

Depending on the physical state of the reaction during this step, the solution may be in the liquid-phase or in a mixture consisting of liquid and solid-phase. The properties of the solvent used during the first step and the molar stoichiometries of the precursor reagents will dictate the physical state of the solution during this step. Additionally, the solvent, precursor stoichiometries, and annealing temperature will also determine the crystalline phases present in the final SSE.

Following synthesis, the solvent removal step is employed to eliminate the liquid medium and isolate the solid-state electrolyte precursor. Common techniques such as rotary evaporation or vacuum drying are often employed to efficiently remove the solvent, leaving behind a concentrated material. Careful control of this step is essential to prevent undesirable side reactions and ensure homogeneity in the resulting solid-state electrolyte precursor.

The synthesized and solvent-free precursor is subjected to annealing, a thermal treatment process that induces crystallization, phase transformation, and the development of the desired crystal structure in the solid-state electrolyte. Annealing conditions, including temperature, duration, and atmosphere, play a critical role in determining the final electrochemical performance of the material. This step is vital for achieving optimal ionic conductivity and stability in the solid-state electrolyte.

3. PRECURSOR REAGENT STOICHIOMETRIES

Excessive studies of Li_2S – P_2S_5 systems processed in acetonitrile (ACN) have provided insight on the importance of molar stoichiometries of the chemical precursors on the system. Accordingly, these stoichiometries can be adjusted to obtain SSEs with unique crystalline phases, such as $\text{Li}_2\text{P}_2\text{S}_6$, $\text{Li}_7\text{P}_3\text{S}_{11}$, or β - Li_3PS_4 when processed in ACN. By adjusting the molar stoichiometries of the precursor reagents the mechanism of formation of the SSE changes depending on the relative abundance of Li_2S to P_2S_5 . The balanced reactions that generate these known crystalline phases from ACN solvent processes are listed in Table 1.

3.1. $50\text{Li}_2\text{S}$ – $50\text{P}_2\text{S}_5$. In ACN, $50\text{Li}_2\text{S}$ – $50\text{P}_2\text{S}_5$ systems have been shown to form a highly soluble $(\text{PS}_3^-)_n$ polymer-like chemical intermediate at temperatures below 180°C .

Table 1. σ , Ionic Conductivities, and Balanced Reactions of the 3 Main $\text{Li}_2\text{S}-\text{P}_2\text{S}_5$ System Processed in Acetonitrile

LPS System	Balanced Reaction	$\sigma_{25^\circ\text{C}}$ (mS cm^{-1})	Reference
50 Li_2S -50 P_2S_5	$\text{Li}_2\text{S} + \text{P}_2\text{S}_5 \rightarrow \text{Li}_2\text{P}_2\text{S}_6$	2.5×10^{-6}	10
70 Li_2S -30 P_2S_5	$3.5\text{Li}_2\text{S} + 1.5\text{P}_2\text{S}_5 \rightarrow \text{Li}_7\text{P}_3\text{S}_{11}$	1.5	11
75 Li_2S -25 P_2S_5	$1.5\text{Li}_2\text{S} + 0.5\text{P}_2\text{S}_5 \rightarrow \beta\text{-Li}_3\text{PS}_4$	0.3	12

However, at elevated temperatures above 220 °C, conversion from $(\text{PS}_3^-)_n$ to a metathiodiphosphate $\text{P}_2\text{S}_6^{2-}$ occurs through calcination and is expressed as $\text{Li}_2\text{P}_2\text{S}_6$ in the crystalline phase of the SSE.¹⁰ Significantly, the highly soluble intermediate formed during the reaction step of this process for 50 Li_2S -50 P_2S_5 systems has only been reported in ACN. The limited information available for this reaction in other solvent types restricts the understanding of this LPS system during suspension synthesis.

3.2. 75 Li_2S -25 P_2S_5 . The initial breakthrough in solution processing SSEs involving the synthesis of a 75 Li_2S -25 P_2S_5 system in tetrahydrofuran (THF) reported by Liu et al⁴ yielded a highly conductive nanoporous material characterized by the metastable $\beta\text{-Li}_3\text{PS}_4$ phase. This phase has also been observed when a 75 Li_2S -25 P_2S_5 system undergoes reaction in other solvents like ACN, 1,2-dimethoxyethane (DME), ethyl acetate (EA). Throughout the reaction step, a complexation phenomenon unfolds, involving interactions between the $\text{Li}_2\text{S}-\text{P}_2\text{S}_5$ precursors and the solvent. In ACN or DME, this intricate process was observed to form an intermediary Li_3PS_4 /solvent complex,¹³ composed of alternating Li_2PS_4^- and Li^+ -solvent layers. Upon heating, this complex undergoes a transformation, giving rise to the $\beta\text{-Li}_3\text{PS}_4$ SSE. This transformation has been conceptualized as a result of uniaxial compression coupled with multidirectional tetrahedral rotation of the PS_4 thiophosphate, as per modeling insights.¹⁴

3.3. 70 Li_2S -30 P_2S_5 . The 70 Li_2S -30 P_2S_5 processed in solution has been observed as having the highest ionic conduction of 1.5 mS cm^{-1} at room temperature when processed in ACN, which is attributed to the crystallization of $\text{Li}_7\text{P}_3\text{S}_{11}$.¹¹ Like the 75 Li_2S -25 P_2S_5 system, the mechanism of formation for a 70 Li_2S -30 P_2S_5 SSE involves a complexation between the $\text{Li}_2\text{S}-\text{P}_2\text{S}_5$ precursors and the solvent.^{10,14-16} A unique characteristic about the synthesis of a 70 Li_2S -30 P_2S_5 system is that it is reliant upon both an insoluble Li_3PS_4 /solvent phase and a soluble (PS_3^-) phase, like observed in a 50 Li_2S -50 P_2S_5 system. This reaction becomes more apparent when analyzing the molar stoichiometries of both the 50 Li_2S -50 P_2S_5 and the 75 Li_2S -25 P_2S_5 systems.

The 70 Li_2S -30 P_2S_5 system does not contain adequate Li_2S for complete synthesis of a $\beta\text{-Li}_3\text{PS}_4$ phase, however it contains excess Li_2S for the formation of the soluble $(\text{PS}_3^-)_n$ phase, as observed in the 50 Li_2S -50 P_2S_5 system. The mechanism of formation for the PS_4^{3-} was proposed to start with the formation of $(\text{PS}_3^-)_n$ in solution, with Li_2S and P_2S_5 in a 1:1 molar ratio. The second step incorporates excess Li_2S into the polymer-type structure of $(\text{PS}_3^-)_n$, thus breaking the P-S-P bridges and leading to the formation of PS_4^{3-} . Subsequent complexation with solvent forms a Li_3PS_4 /solvent, which has been shown to be insoluble when using ACN.¹⁰ Since the conductivity of a 70 Li_2S -30 P_2S_5 is reliant upon the formation of $\text{Li}_7\text{P}_3\text{S}_{11}$, the formation of both PS_4^{3-} and $\text{P}_2\text{S}_7^{4-}$ is critical.

One proposed mechanism of formation for $\text{P}_2\text{S}_7^{4-}$ states that PS_4^{3-} is incorporated into the $(\text{PS}_3^-)_n$ chain, resulting in chain

cleavage and stabilizing $\text{P}_2\text{S}_7^{4-}$ as seen in Figure 2. Upon annealing, PS_4^{3-} and $\text{P}_2\text{S}_7^{4-}$ crystallize with 7 Li^+ to form $\text{Li}_7\text{P}_3\text{S}_{11}$.

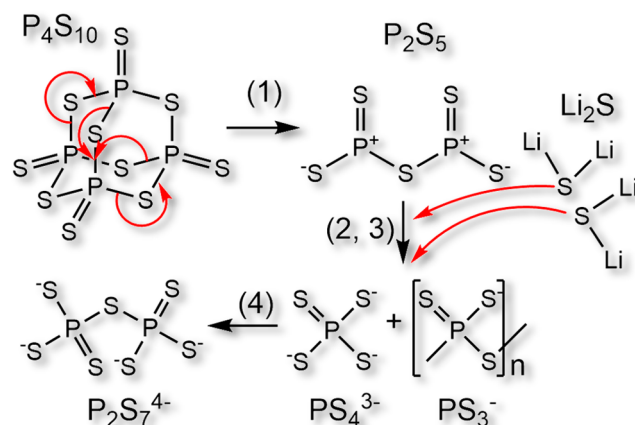


Figure 2. (1) P_4S_{10} monomerizes at elevated temperatures to P_2S_5 . (2, 3) Li_2S reacts with the unstable P_2S_5 to stabilize the soluble polymer-like PS_3^- and PS_4^{3-} . (4) PS_3^- and PS_4^{3-} join to form $\text{P}_2\text{S}_7^{4-}$. Adapted from Rosero et al, 2018.¹⁰

Another reported possible mechanism of formation for $\text{Li}_7\text{P}_3\text{S}_{11}$ suggests that the intermediate $\text{Li}_2\text{P}_4\text{S}_{11}$ is initially formed with Li_2S and P_2S_5 in a 1:2 molar ratio, respectively. A lone pair of electrons belonging to the sulfur in Li_2S attacks a P-S bond in the adamantane-like structure of P_4S_{10} , and partially opens the cage-like structure. A subsequent nucleophilic attack of Li_2S further opens the structure and forms $\text{Li}_4\text{P}_4\text{S}_{12}$. Further integration of Li_2S into the reaction separates insoluble Li_3PS_4 from soluble $\text{Li}_4\text{P}_2\text{S}_7$ in solution, as seen in Figure 3. Following solvent removal, the annealing step promotes the crystallization of $\text{Li}_7\text{P}_3\text{S}_{11}$.¹⁶

4. SOLVENT SELECTION

A key aspect of solution-based suspension synthesis of SSEs is choosing a solvent in which to perform the reaction. Chemical properties of the solvent such as polarity and molecular composition have both shown to influence solution processes. Highly polar solvents like NMF, completely dissociate the LPS system, while solvents with less polarity like ACN tend to form LPS/solvent complexes. Solvents containing oxygen tend to be problematic as they have been reported to introduce impurities into SSEs, as discussed later on LPSC systems. Likewise, polar solvents that exhibit acidic behavior toward Li_2S or P_2S_5 are particularly hazardous as they can produce toxic H_2S gas, as observed when reacted with water.

The interactions between LPS precursors, intermediates, and the solvent also play a pivotal role in determining particle morphology^{17,18} and the overall ionic conductivity of the SSE. A variety of solvents have been analyzed with solution processing techniques of SSEs including acetates, nitriles, ethers, and amides. Figure 4 illustrates reported solvents used during suspension synthesis of LPS systems and their corresponding molar proportion of Li_2S .

Noticeable in Figure 4, ACN has synthesized SSEs with both the highest and the lowest ionic conductivities of the reported LPS systems at 0.9 and 0.002 mS cm^{-1} , respectively. This difference is attributed to the molar stoichiometric difference between the two LPS systems. However, ACN remains as the

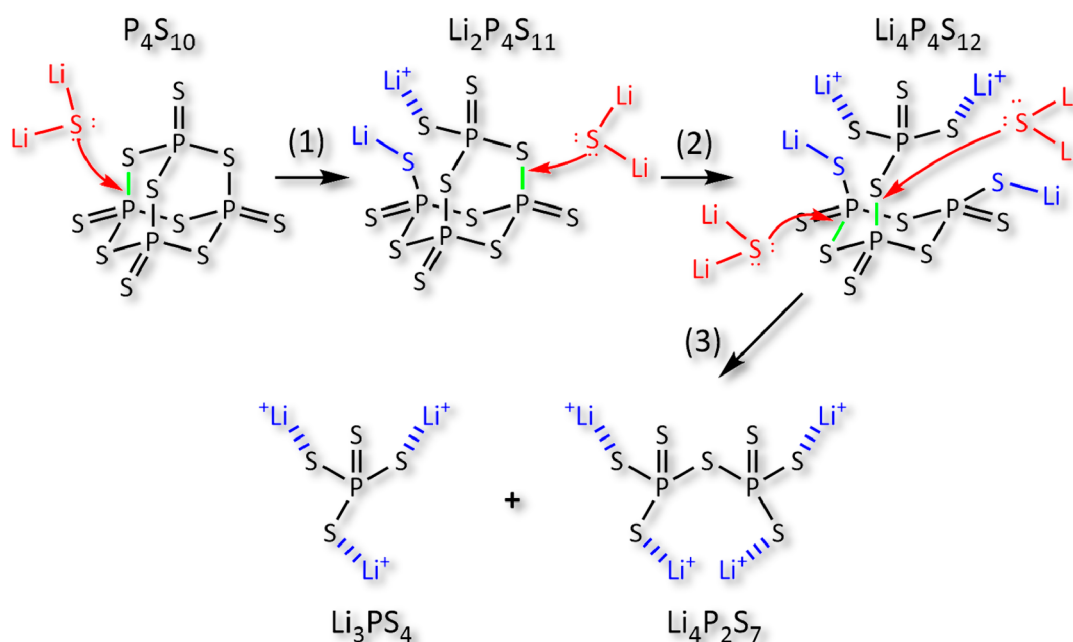


Figure 3. (1) Li_2S reacts with P_4S_{10} to form $\text{Li}_2\text{P}_4\text{S}_{11}$. (2) Additional Li_2S reacts with $\text{Li}_2\text{P}_4\text{S}_{11}$ to form $\text{Li}_4\text{P}_4\text{S}_{12}$. (3) More Li_2S reacts with $\text{Li}_4\text{P}_4\text{S}_{12}$ to form Li_3PS_4 and $\text{Li}_4\text{P}_2\text{S}_7$. Adapted from Wang et al, 2020.¹⁶

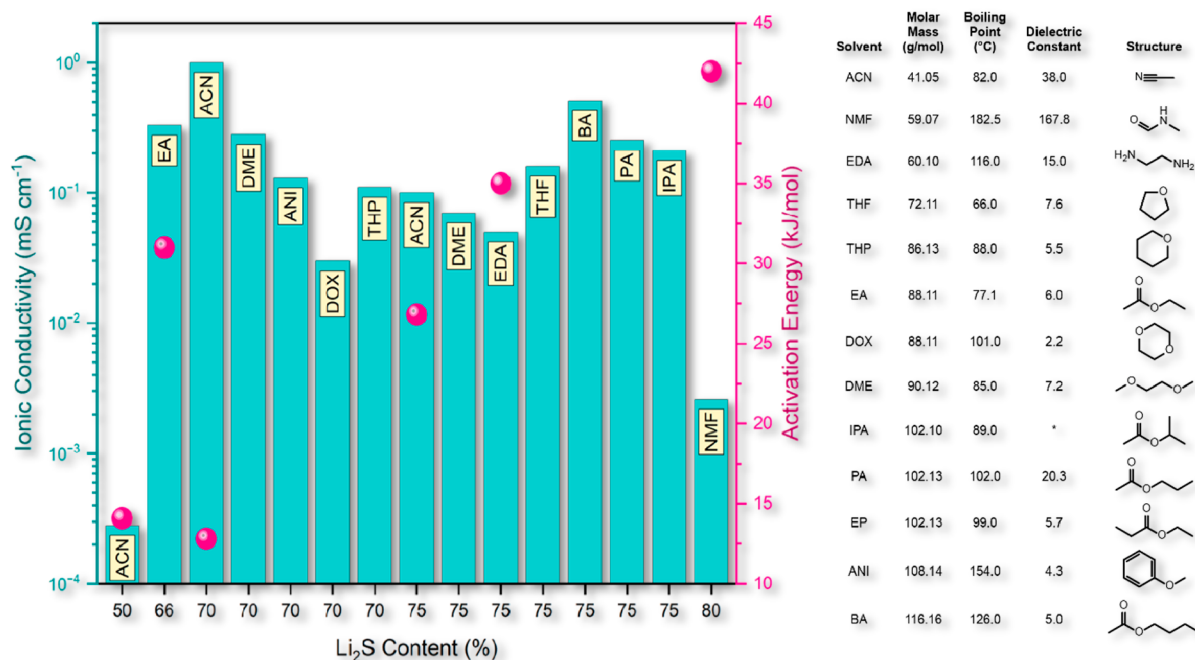


Figure 4. Ionic conductivities and reported activation energies of SSEs synthesized in organic solvents with respective $\text{Li}_2\text{S}:\text{P}_2\text{S}_5$ content: 50:50 in acetonitrile (ACN),¹⁰ 66:33 ethyl acetate (EA),¹² 70:30 in acetonitrile (ACN),¹¹ 70:30 in 1,2-dimethoxyethane (DME),¹⁹ 70:30 in anisole (ANI),¹⁹ 70:30 in 1,4-dioxane (DOX),¹⁹ 70:30 in tetrahydropyran (THP),¹⁹ 75:25 in ACN,¹⁰ 75:25 in DME,¹⁴ 75:25 in ethylenediamine (EDA),²⁰ 75:25 in tetrahydrofuran (THF),⁴ 75:25 in butyl acetate (BA),²¹ 75:25 in propyl acetate (PA),²¹ 75:25 in isopropyl acetate (IPA),²¹ 80:20 in *N*-methylformamide (NMF).²² Reactions reported without activation energies are referenced only for molar composition and ionic conductivity of the produced SSE. *Not reported.

solvent that synthesizes LPS SSEs with the highest ionic conductivity and the lowest activation energy. Comparatively, most of the other solvents reported synthesized SSEs with ionic conductivities of almost a full order of magnitude less than ACN, with a few exceptions such as acetates. Likewise, BA was reported to synthesize an SSE with higher ionic

conductivity than the other acetates at the same 75:25 molar ratios.

A trend that was reported by Yamamoto et al. when synthesizing LPS SSEs in acetate solvents was that the boiling point negatively correlated to ionic conductivity of the final SSE. They suggested that the lower the boiling point of the acetate the easier solvent removal occurs from the SSE, which

leads to a purer product with higher ionic conductivity.²¹ However, this trend has not been reported in other types of solvents.

Aside from the previous assessments of ACN and the acetate solvents, information regarding the types of solvent reported appears ambiguous. An evaluation of solvent polarity, size, acidity, molecular composition, and donor number could offer more insight into these reports. The polarity of a solvent can be illustrated based on its ability to insulate charges of other molecules, also referred to as its dielectric constant. Figure 5

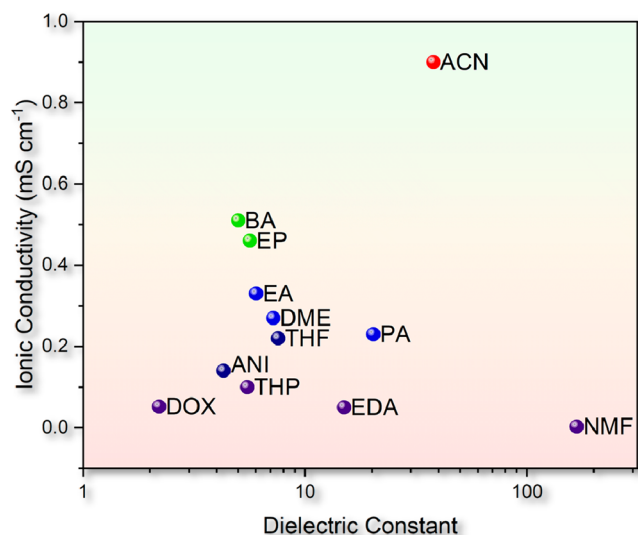


Figure 5. Highest ionic conductivity reported from LPS SSEs versus the dielectric constant of each solvent used during the reaction step of the solution process from Figure 4. Dielectric constant of each respective solvent offers a numerical visualization of the polarity of the solvent; however, there is no apparent correlation with the overall ionic conductivity of the synthesized SSE and the dielectric constant of the solvent. The significant difference between the values of the dielectric constants of DOX, THP, EDA, and NMF coupled with the lower ionic conductivity of their respective SSE products suggests that other chemical properties associated with these solvents, or a combination of chemical properties and process conditions influence the synthesis of the LPS SSE more than only the polarity of the solvent.

expresses the solvents reported in Figure 4 along with the highest corresponding ionic conductivity reported from the SSEs synthesized and the dielectric constant of the solvent, apart from IPA because its dielectric constant has not been reported.

The trend presented by Yamamoto is apparent, to include ethyl acetate. As the polarity of the acetate solvents increase, the ionic conductivity of the SSE decreases. Thus, correlating the boiling point of acetate solvents and ionic conductivity of the respective SSE. However, the correlation between boiling point and ionic conductivities is likely not the case with solvents other than the acetates. NMF is a highly polar solvent, which has a solubilizing effect on LPS systems as reported by Tatsumisago et al.²² The synthesis of β - Li_3PS_4 and $\text{Li}_7\text{P}_3\text{S}_{11}$ in LPS systems is reliant upon complexation between LPS precursors and the solvent during suspension synthesis, as discussed later in section 3. Therefore, the complete dissociation of the LPS system during synthesis will likely have a negative effect on the ionic conductivity of the SSE.

Not all polar solvents have this effect on the LPS synthesis. ACN has a dielectric constant of 38, making it more polar than most of the solvents that were evaluated, yet the highest ionic conductivities of SSEs reported were synthesized in ACN. There are a few characteristics about ACN that make it more unique than most other solvents. ACN is a polar-aprotic solvent and the smallest nitrile species. The aprotic property of ACN, means that it cannot reduce LPS to form H_2S , while the nitrile functional group offers sufficient polarity to perform LPS synthesis and highly conductive SSEs. Little research has explored the effect that the molecular size of the solvent has on the suspension synthesis of LPS SSEs. However, Rosero et al.'s 2021 report on the formation of β - Li_3PS_4 using ACN and DME shows that the size of the solvent does have influence on the LPS precursor/solvent complex that is formed because the larger solvents accommodate more molecular volume.¹⁴

Furthermore, approaches to solvent selection using higher donor numbers and polarity have been effective at appropriately choosing solvents that can activate reactions of lithium polysulfides, but this is not necessarily true with LPS systems. Matsuda et al. explains that the high reactivity of a LPS system in ACN cannot completely be attributed to the donor number, because ACN has a relatively low donor number.¹⁹ Additionally, Yamamoto et al. showed that a negative correlation between the polarity of certain acetate solvents and the ionic conductivity of the SSE for Li_3PS_4 systems can occur due to weak solvent/precursor interactions.²¹ Of all the reported solvents, ACN has been shown to synthesis LPS SSEs with the highest ionic conductivity and lowest activation energies. Contrarily, there still lacks much information regarding the chemistries of these solution processes and how they are facilitated by solvent/reagent interactions. Properties such as polarity and molecular composition of the solvent are important when performing solution-based suspension synthesis of LPS systems. As well, other factors such as boiling temperature, reactivity, and toxicity should also be considered when designing a solution process for LPS SSEs.

5. FACTORS THAT INFLUENCE IONIC CONDUCTIVITY

Apart from selecting a desirable reagent stoichiometry between Li_2S – P_2S_5 and a solvent to perform the solution-based suspension synthesis, factors such as reaction conditions, impurities, and morphology of SSEs can influence the overall performance of the reaction and the properties of the SSEs produced.

Lithium sulfide is known to be reactive with moisture in the air, releasing hydrogen sulfide gas when reacted with water. Tufail et al. studied the oxide doping on lithium phosphorus sulfide (LPS) systems and the effects of humid air on $\text{Li}_7\text{P}_3\text{S}_{11}$ electrolytes. They showed that the SSE reacts with water to produce H_2S gas and the oxidized thiophosphate anions PO_3^{3-} and 2HO-PS_3^{2-} , resulting a reduction in electrochemical performance of the SSE.²³ This oxidation process is illustrated in Figure 6.

Subsequent studies in the sulfide electrolytic system $\text{Li}_6\text{PS}_5\text{Cl}$ demonstrated how oxygenated organic solvents like tetrahydrofuran and ethanol in the presence of LiCl can react with the chemical precursor P_2S_5 in a nucleophilic reaction incorporating oxygen and forming lithium phosphates.²⁴ Ring opening reactions of cyclic ethers like THF in acidic aqueous conditions are well-known, which can lead to diols and alkyl halides through a 3-step reaction: protonation, $\text{S}_\text{N}2$ reaction, deprotonation. In the report of Matsuda et al., they showed

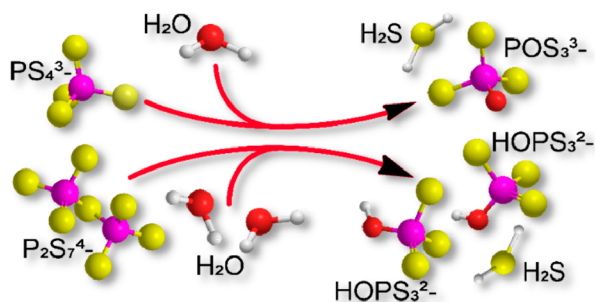


Figure 6. Anion thiophosphates PS_4^{3-} and $\text{P}_2\text{S}_7^{4-}$ oxidized by water to form H_2S gas, POS_3^{3-} , and HOPS_3^{2-} . Adapted from Tufail et al., 2021.²³

that the ring opening of THF is stabilized from an interaction between both ethanol and LiCl. The strong electronegative character of Cl^- attracts the H of the formed hydroxide exposing the O^δ . The oxygen then attacks the phosphorus of P_2S_5 leading to oxidation of the phosphorus to PO_4^{3-} , Figure 7. The same report illustrated a similar mechanism using propanethiol, LiCl, and THP which also led to the formation of PO_4^{3-} , thus introducing impurities into the SSE and adversely impacting the performance of the electrolyte.

The solvent facilitated oxidation in $\text{Li}_2\text{S}-\text{P}_2\text{S}_5$ systems is less explored than its' cousin, the argyrodite-type SSE, however these reaction systems share precursor chemicals such as Li_2S and P_2S_5 , as well as types of solvents, which lends credence to the postulate that oxygenated solvents have the capability to oxidize precursors and intermediates during reactions of $\text{Li}_2\text{S}-\text{P}_2\text{S}_5$ systems. Subsequently, these reactions will lead to impurities in the SSE and reduced electrochemical performance.

The reduction or prevention of oxide impurities from occurring in sulfide SSEs is pivotal when generating high-performance electrolytes, however other impurities formed from undesirable reactions can occur from excess temperatures even without contaminated solvents or exposure to air.

There exists little information on the effects of reaction temperatures in solution-based suspension synthesis of $\text{Li}_2\text{S}-\text{P}_2\text{S}_5$ SSEs, with most reported experiments occurring between 25 and 60 °C coupled with ultrasonic irradiation or magnetic stirring.^{11,15,16,19,25,26} However, annealing temperature studies have been performed on sulfide SSEs from both the mechanical and solution-based suspension synthesis. Wei et al. performed annealing studies on the $70\text{Li}_2\text{S}-30\text{P}_2\text{S}_5$ system synthesized via mechanical ball milling. During their experi-

ments, they observed that the highest ionic conductivity was optimal at an annealing temperature of 250 °C. Above this temperature they reported the loss of sulfur resulting in the formation of a notable amount of $\text{Li}_4\text{P}_2\text{S}_6$ within the SSE.²⁷ This sublimation of sulfur and generation of undesirable $\text{Li}_4\text{P}_2\text{S}_6$ impurity has been observed in many instances, all yielding a reduction in ionic conductivity of the synthesized SSEs.^{16,26-28}

$\text{Li}_4\text{P}_2\text{S}_6$ can be easily identified in the $\text{Li}_2\text{S}-\text{P}_2\text{S}_5$ system by Raman and nuclear magnetic resonance spectroscopy. $\text{Li}_2\text{S}-\text{P}_2\text{S}_5$ systems with 70:30 and 75:25 respective molar stoichiometries containing $\text{Li}_4\text{P}_2\text{S}_6$ produce a visible Raman band at approximately 390 cm^{-1} in addition to the bands representing PS_4^{3-} ($417-419\text{ cm}^{-1}$) and $\text{P}_2\text{S}_7^{4-}$ ($400-404\text{ cm}^{-1}$). Raman spectra of ideal $\text{Li}_2\text{S}-\text{P}_2\text{S}_5$ SSEs devoid of $\text{Li}_4\text{P}_2\text{S}_6$ are illustrated in Figure 8a (50:50), 8c (70:30), and 8e (72,25). Corresponding spectra for samples containing $\text{Li}_4\text{P}_2\text{S}_6$ with 70:30 and 75:25 (Figure 8d and 8f) molar stoichiometries show the presence of the Raman band associated with $\text{P}_2\text{S}_6^{4-}$, which is commonly observed in samples annealed in excess of 250 °C. The $50\text{Li}_2\text{S}-50\text{P}_2\text{S}_5$ system is the only system that may require the additional verification using solid-state ^{31}P NMR because a primary Raman band for $\text{P}_2\text{S}_6^{4-}$ and $\text{P}_2\text{S}_6^{2-}$ occur at relatively similar positions between 385 and 390 cm^{-1} , as visualized in Figure 8b and 8d.

Another reported benefit of solution-based suspension synthesis of sulfide SSEs is the ability to have better control over particle size and morphology than mechanical processing. Liu et al.'s reported SSE particles synthesized in THF obtained a uniform rectangular morphology ranging in size from 10 to $30\text{ }\mu\text{m}$,⁴ similar to the rectangular morphology of SSE particles synthesized in DME by Rosero et al.¹⁴ Liang et al. was able to synthesize nanoflake particles from $75\text{Li}_2\text{S}-25\text{P}_2\text{S}_5$ with controlled thickness between 8 and $50\text{ }\mu\text{m}$ in ACN by a dissolution-precipitation technique. By decreasing the concentration of the SSE during the dissolution-precipitation process, nanoflake layers would precipitate with reduced thickness onto the active material being coated.¹³

Zhou et al. designed a suspension synthesis method that can tailor amorphous SSE particle size for systems with 70:30 and 75:25 molar proportions of $\text{Li}_2\text{S}:\text{P}_2\text{S}_5$. In this method, they showed that by decreasing the reaction concentration of LPS in EA from 40 to 10 mg/mL and selectively tuning the evaporation temperature of the solvent between 80 and 150 °C, the SSE particle size could be controlled down to 100 nm in size. However, Zhou et al.'s report highlighted an important aspect of SSE particle size and morphology; the highest ionic

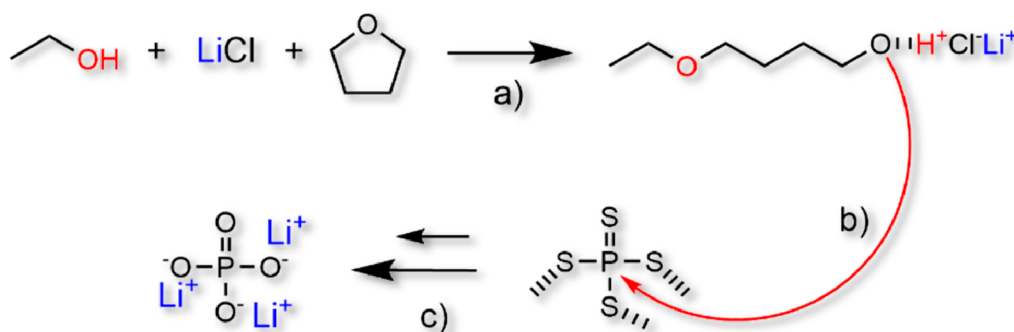


Figure 7. Solvent facilitated oxidation of P_2S_5 from nucleophile intermediate in 3-step mechanism: (a) Ring opening of THF stabilized by LiCl and ethanol, (b) nucleophilic substitution of sulfur for oxygen in P_2S_5 , and (c) full oxidation of P_2S_5 to PO_4^{3-} units. Adapted from Matsuda et al.²⁴

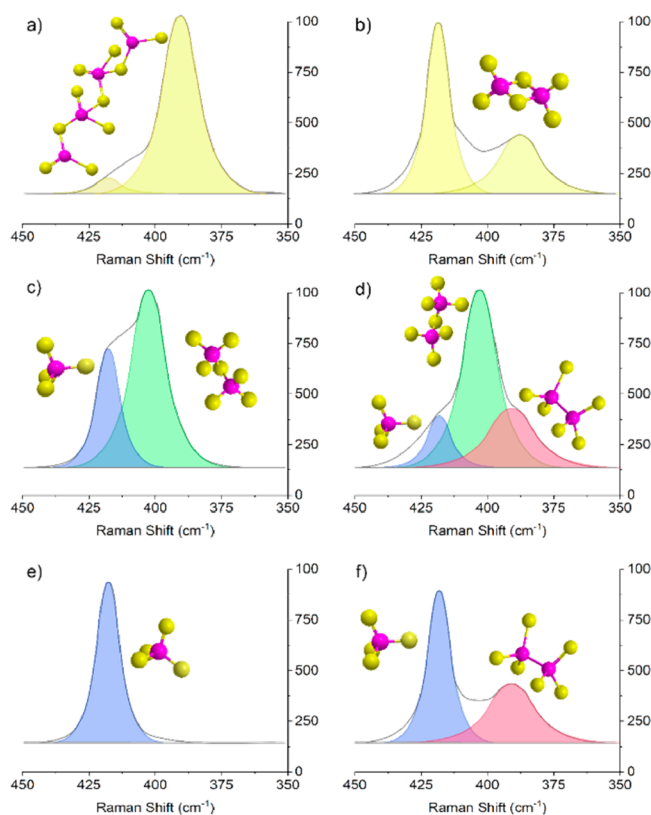


Figure 8. Raman spectra between 350 and 450 cm^{-1} for a $50\text{Li}_2\text{S}-50\text{P}_2\text{S}_5$ mixture (a) in ACN and (b) after annealing at 220 $^\circ\text{C}$; 10 $70\text{Li}_2\text{S}-30\text{P}_2\text{S}_5$ synthesized in ACN and annealed at 220 $^\circ\text{C}$ (c) without $\text{P}_2\text{S}_6^{4-}$ contamination and (d) with $\text{P}_2\text{S}_6^{4-}$ contamination; 28 $75\text{Li}_2\text{S}-25\text{P}_2\text{S}_5$ synthesized in ACN and annealed at 220 $^\circ\text{C}$ (e) without $\text{P}_2\text{S}_6^{4-}$ contamination and (f) with $\text{P}_2\text{S}_6^{4-}$ contamination.

conductivity is not always observed from the SSEs with the smallest particle size. They suggest that the smaller the particle size, the more grain boundaries may exist, which can decrease the ionic conductivity, so there should be a balance between particle size and conductivity of the SSE to have good mechanical and electrochemical properties.¹⁷

Our Perspective. Since the introduction of solution-based suspension synthesis of SSEs, research into this field has only progressed moderately and there still lacks fundamental information about these reaction processes. From the investigations reported in this review there are some key takeaways worth further discussion.

The most reported reaction of LPS in suspension synthesis is $75\text{Li}_2\text{S}-25\text{P}_2\text{S}_5$, from which the SSEs synthesized have almost all been identified as $\beta\text{-Li}_3\text{PS}_4$. Even though most of the reported experiments identified the same phase in the final SSE, the ionic conductivities varied by an order of magnitude or more in some cases, which may be an effect of varied SSE morphology and size. The chemical properties of the solvents have been shown to control the morphology and size of the SSE particles which both contribute to the ionic conductivity. The interaction between most of the reported solvents and the precursors are still yet to be examined in detail, however aprotic solvents with low boiling points and moderate polarity, such as ACN and acetates have been shown to produce LPS SSEs with the highest ionic conductivity, all while being able to control the morphology and size of the SSE particles.

The reactions of LPS in suspension synthesis in varied molar stoichiometries necessitate further investigation. For the LPS system $50\text{Li}_2\text{S}-50\text{P}_2\text{S}_5$ reaction in solvent, there has only been 1 report of an experiment performed and it was in ACN. This is also the only known proportion of LPS to have a soluble intermediate and has yet to be reported in other solvents. Like the $50\text{Li}_2\text{S}-50\text{P}_2\text{S}_5$ system, the $70\text{Li}_2\text{S}-30\text{P}_2\text{S}_5$ could use further evaluation in different solvent and reaction conditions. There currently exist two proposed reaction mechanisms for formation of the $\text{Li}_7\text{P}_3\text{S}_{11}$ phase that is synthesized in the $70\text{Li}_2\text{S}-30\text{P}_2\text{S}_5$, both of which are described in ACN. This is also the highest ionically conductive LPS that has been synthesized.

To synthesize highly conductive SSEs from LPS, control over the reaction conditions is imperative. From the reported experiments the conditions for SSEs with the highest ionic conductivities were stirred for 24 h at 50 $^\circ\text{C}$ or ultrasonicated for 30 min at 60 $^\circ\text{C}$. As Zhou et al. discussed, the solvent removal step is critical for controlling the final particle size.¹⁷ A rapid solvent removal at 100 $^\circ\text{C}$ was used to synthesize particles down to 8 nm from a 10 mg/mL reaction solution, albeit the vacuum pressure was not reported. Lastly, the temperature of the final annealing of LPS SSEs should not exceed 250 $^\circ\text{C}$, as it can cause the evolution of sulfur and cause the formation of the low ionic conductive species $\text{Li}_4\text{P}_2\text{S}_6$.

An optimal reaction based on the reported data would be a $70\text{Li}_2\text{S}-30\text{P}_2\text{S}_5$ in a 10–20 mg/mL reaction concentration in ACN or EA. This would react for 24 h at 50 $^\circ\text{C}$, dry at 100 $^\circ\text{C}$, and then anneal at a temperature less than 250 $^\circ\text{C}$. The synthesized SSE should obtain a high ionically conductive phase of $\text{Li}_7\text{P}_3\text{S}_{11}$ with an amorphous particle size between 100 and 200 nm.

CONCLUSION

In the rapidly evolving field of energy storage, solid-state batteries are likely the next generation technology that can offer improved performance and safety over current conventional lithium-ion batteries. Sulfide-based solid-state electrolytes are contenders for enabling breakthroughs in solid-state battery research with LPS systems exhibiting exceptional electrochemical and mechanical properties.

Current processing techniques for the generation of sulfide SSEs are energetically consumptive with prolonged processing times. However, solution-based suspension synthesis LPS SSEs mitigates time and energy constraints by reducing reaction temperatures and processing times. Even though this type of solution processing is likely scalable, the underlying reaction mechanism associated with these synthesis techniques are still not well-understood. This review briefly discussed what solution-based suspension synthesis of LPS systems is and how it can be performed. Here we also evaluated key factors that influence the process and performance of final SSEs including molar stoichiometries, solvent selectivity, reaction conditions, impurities, and SSE morphology. Lastly, we provide our perspective on what an ideal solution-based suspension synthesis would be based on combined reported data.

Additional studies are needed to help understand the reaction conditions including how temperature influences chemical intermediates in solution and how solvents help facilitate these reactions in different molar stoichiometries of LPS precursors.

AUTHOR INFORMATION

Corresponding Author

Nataly Carolina Rosero-Navarro – Instituto de Cerámica y Vidrio – CSIC, 28049 Madrid, Spain; orcid.org/0000-0001-6838-2875; Email: rosero@icv.csic.es

Author

Zachary Warren – Instituto de Cerámica y Vidrio – CSIC, 28049 Madrid, Spain; Department of Chemistry, Texas A&M University-Commerce, Commerce, Texas 75428, United States; orcid.org/0000-0002-4246-8598

Complete contact information is available at:

<https://pubs.acs.org/10.1021/acsomega.4c03784>

Notes

The authors declare no competing financial interest.

Biographies



Zachary Warren is a predoctoral researcher completing his PhD thesis under the supervision of Dr. Nataly Carolina Rosero-Navarro at the Instituto de Cerámica y Vidrio, part of the Consejo Superior de Investigaciones Científicas in Madrid, Spain. He completed his undergraduate and graduate education in Chemistry and Biochemistry from the University of Texas at Tyler, Arizona State University, and Texas A&M University-Commerce. In his current research, Zachary focuses on the reaction chemistries underlying solution-based processing techniques of sulfide solid electrolytes for solid-state batteries. His projects include electrolyte synthesis, cathode material preparation, and battery performance analysis. Prior to joining the Instituto de Cerámica y Vidrio, he worked at Eastman Chemical, where he developed and performed advanced analytical techniques related to the synthesis of organic solvents, thus building a strong foundation of research and practical laboratory experience.



Nataly Carolina Rosero-Navarro is Tenured Scientist of Instituto de Cerámica y Vidrio (Institute of Ceramic and Glass) at The Spanish National Research Council CSIC, Spain. She is also a Guest Associate Professor of Division of Applied Chemistry, Faculty of Engineering at Hokkaido University, Japan. She got Degree of Doctor in Chemistry Science from University Autonomous of Madrid, Spain in 2011. Rosero-Navarro's research career is based on the implementation of the solution processes for the synthesis and characterization of inorganic (glassy and crystalline) and organic-inorganic materials for environmental and energy applications. Particularly, she has accumulated a recognized experience in the design of hybrid and inorganic coatings with unique corrosion inhibition, bioactive and chemical-resistance properties providing significant knowledge in the area of ecofriendly sol-gel coatings and multilayer systems. She has also implemented novel soft chemical routes to prepare protonic hybrid membranes, sulfide and oxide solid electrolytes, materials for electrode/electrolyte interfaces and composites electrodes for all-solid-state batteries and, electrocatalysts for fuel cells and metal-air batteries providing new insights and concepts for the improvement of energy generation and storages. She has received Awards including WinGS (Women in Global Science) Award in 2017 and Ulrich Award in 2022. Her long-term goal includes the design and synthesis of inorganic and hybrid materials for the next "green" energy generation and storage.

ACKNOWLEDGMENTS

This research work is part of PIE project "Innovative and Designed (Electro)-Chemistry, All-in-One for Lithium Sulfide Solid Electrolytes" (IDEAL-Li), reference 20226AT009 supported by The Spanish National Research Council (CSIC). Financial support of this work through Ramon y Cajal Grant No. RYC2020-029909-I of The Spanish State Research Agency to N.C. Rosero-Navarro.

REFERENCES

- (1) Kamaya, N.; et al. A lithium superionic conductor. *Nat. Mater.* **2011**, *10* (9), 682–6.
- (2) Seino, Y.; Ota, T.; Takada, K.; Hayashi, A.; Tatsumisago, M. A sulphide lithium super ion conductor is superior to liquid ion conductors for use in rechargeable batteries. *Energy Environ. Sci.* **2014**, *7* (2), 627–631.
- (3) Kato, Y.; et al. High-power all-solid-state batteries using sulfide superionic conductors. *Nature*. **2016**, *1* (4), 16030.
- (4) Liu, Z.; et al. Anomalous high ionic conductivity of nanoporous beta-Li3PS4. *J. Am. Chem. Soc.* **2013**, *135* (3), 975–8.
- (5) Teragawa, S.; Aso, K.; Tadanaga, K.; Hayashi, A.; Tatsumisago, M. Formation of Li2S-P2S5 Solid Electrolyte from N-Methylformamide Solution. *Chem. Lett.* **2013**, *42* (11), 1435–1437.
- (6) Wang, Y.; Liu, Z.; Zhu, X.; Tang, Y.; Huang, F. Highly lithium-ion conductive thio-LISICON thin film processed by low-temperature solution method. *J. Power Sources* **2013**, *224*, 225–229.
- (7) Teragawa, S.; Aso, K.; Tadanaga, K.; Hayashi, A.; Tatsumisago, M. Liquid-phase synthesis of a Li3PS4 solid electrolyte using N-methylformamide for all-solid-state lithium batteries. *Journal of Materials Chemistry A* **2014**, *2* (14), 5095.
- (8) Tu, T. A.; Toan, T. V.; Anh, L. T.; Thang, L. V.; Phuc, N. H. H. Synergic effect of CaI(2) and LiI on ionic conductivity of solution-based synthesized Li(7)P(3)S(11) solid electrolyte. *RSC Adv.* **2024**, *14* (9), 5764–5770.
- (9) Rajagopal, R.; Subramanian, Y.; Jung, Y. J.; Kang, S.; Ryu, K.-S. Rapid Synthesis of Highly Conductive Li6PS5Cl Argyrodite-Type Solid Electrolytes Using Pyridine Solvent. *ACS Appl. Energy Mater.* **2022**, *5* (8), 9266–9272.
- (10) Calpa, M.; Rosero-Navarro, N. C.; Miura, A.; Terai, K.; Utsuno, F.; Tadanaga, K. Formation Mechanism of Thiophosphate Anions in

the Liquid-Phase Synthesis of Sulfide Solid Electrolytes Using Polar Aprotic Solvents. *Chem. Mater.* **2020**, *32* (22), 9627–9632.

(11) Calpa, M.; Rosero-Navarro, N. C.; Miura, A.; Tadanaga, K. Instantaneous preparation of high lithium-ion conducting sulfide solid electrolyte Li₇P₃S₁₁ by a liquid phase process. *RSC Adv.* **2017**, *7* (73), 46499–46504.

(12) Phuc, N. H. H.; Totani, M.; Morikawa, K.; Muto, H.; Matsuda, A. Preparation of Li₃PS₄ solid electrolyte using ethyl acetate as synthetic medium. *Solid State Ionics* **2016**, *288*, 240–243.

(13) Wang, H.; Hood, Z. D.; Xia, Y.; Liang, C. Fabrication of Ultrathin Solid Electrolyte Membranes of β-Li₃PS₄ Nanoflakes by Evaporation-Induced Self-Assembly for All-Solid-State Batteries. *J. Mater. Chem. A* **2016**, *4*, 8091.

(14) Calpa, M.; et al. Formation Mechanism of beta-Li(3)PS(4) through Decomposition of Complexes. *Inorg. Chem.* **2021**, *60* (10), 6964–6970.

(15) Wang, Y.; et al. Mechanism of Formation of Li₇P₃S₁₁ Solid Electrolytes through Liquid Phase Synthesis. *Chem. Mater.* **2018**, *30* (3), 990–997.

(16) Wang, Z.; et al. Reaction mechanism of Li₂S–P₂S₅ system in acetonitrile based on wet chemical synthesis of Li₇P₃S₁₁ solid electrolyte. *Chem. Eng. J.* **2020**, *393*, 124706.

(17) Zhou, J.; et al. Wet-chemical synthesis of Li₇P₃S₁₁ with tailored particle size for solid state electrolytes. *Chem. Eng. J.* **2022**, *429*, 132334.

(18) Xu, J.; Wang, Q.; Yan, W.; Chen, L.; Li, H.; Wu, F. Liquid-phase synthesis of Li₂S and Li₃PS₄ with lithium-based organic solutions. *Chinese Physics B* **2022**, *31* (9), 098203.

(19) Gamo, H.; Nagai, A.; Matsuda, A. The effect of solvent on reactivity of the Li(2)S–P(2)S(5) system in liquid-phase synthesis of Li(7)P(3)S(11) solid electrolyte. *Sci. Rep* **2021**, *11* (1), 21097.

(20) Ito, A.; Kimura, T.; Sakuda, A.; Tatsumisago, M.; Hayashi, A. Liquid-phase synthesis of Li₃PS₄ solid electrolyte using ethylenediamine. *J. Sol-Gel Sci. Technol.* **2022**, *101* (1), 2–7.

(21) Yamamoto, K.; et al. High Ionic Conductivity of Liquid-Phase-Synthesized Li₃PS₄ Solid Electrolyte, Comparable to That Obtained via Ball Milling. *ACS Appl. Energy Mater.* **2021**, *4* (3), 2275–2281.

(22) Teragawa, S.; Aso, K.; Tadanaga, K.; Hayashi, A.; Tatsumisago, M. Preparation of Li₂S–P₂S₅ solid electrolyte from N-methylformamide solution and application for all-solid-state lithium battery. *J. Power Sources* **2014**, *248*, 939–942.

(23) Khurram Tufail, M. Insight on air-induced degradation mechanism of Li₇P₃S₁₁ to design a chemical-stable solid electrolyte with high Li₂S utilization in all-solid-state Li/S batteries. *Chem. Eng. J.* **2021**, *425*, 130535.

(24) Indrawan, R. F.; Gamo, H.; Nagai, A.; Matsuda, A. Chemically Understanding the Liquid-Phase Synthesis of Argyrodite Solid Electrolyte Li₆PS₅Cl with the Highest Ionic Conductivity for All-Solid-State Batteries. *Chem. Mater.* **2023**, *35* (6), 2549–2558.

(25) Gamo, H.; Nishida, J.; Nagai, A.; Hikima, K.; Matsuda, A. Solution Processing via Dynamic Sulfide Radical Anions for Sulfide Solid Electrolytes. *Advanced Energy and Sustainability Research* **2022**, DOI: 10.1002/aesr.202200019.

(26) Ito, S.; Nakakita, M.; Aihara, Y.; Uehara, T.; Machida, N. A synthesis of crystalline Li₇P₃S₁₁ solid electrolyte from 1,2-dimethoxyethane solvent. *J. Power Sources* **2014**, *271*, 342–345.

(27) Wei, J.; et al. Influence of annealing on ionic transfer and storage stability of Li₂S–P₂S₅ solid electrolyte. *J. Power Sources* **2015**, *294*, 494–500.

(28) Calpa, M.; Rosero-Navarro, N. C.; Miura, A.; Tadanaga, K. Preparation of sulfide solid electrolytes in the Li₂S–P₂S₅ system by a liquid phase process. *Inorganic Chemistry Frontiers* **2018**, *5* (2), 501–508.